Zoological Archives: An International Journal
ISSN: 3117-695X
https://stanfordgroup.org/index.php/ZAIJ/issue/archive

Skeletal Variation and Evolution in Felids

Anna Petrov[1], Matteo Popescu[2], Amelia Garcia[3]

[1] Senior Lecturer, Department of Computer Science, Mediterranean Institute of Technology, Rome, Italy. Email: anna.petrov852@yahoo.com | ORCID: 7718-5429-7184-7878
[2] Postdoctoral Researcher, Department of Artificial Intelligence, Baltic AI Research University, Tallinn, Estonia. Email: matteo.popescu613@yahoo.com | ORCID: 8068-1728-9932-0681
[3] Assistant Professor, Institute of Intelligent Systems, European Institute of AI, Berlin, Germany. Email: amelia.garcia728@yahoo.com | ORCID: 7625-2652-3353-7547

ABSTRACT

The Family Felidae -- 41 described species spanning body masses from 1.5 kg (black-footed cat Felis nigripes) to 320 kg (tiger Panthera tigris) -- represents one of the most ecologically successful and morphologically stereotyped mammalian radiations: despite the extraordinary body size range, all living felids share a highly conserved carnivore body plan adapted for stalking-ambush predation, with skeletal proportions constrained by the biomechanical requirements of prey capture, killing, and consumption. Yet within this conserved plan, substantial interspecific variation exists in skull morphology (particularly the facial region and dentition), limb proportions, and vertebral column characteristics that reflect both phylogenetic history and ecological adaptation to diverse prey types and hunting environments. This study presents the most comprehensive geometric morphometric analysis of felid skeletal variation yet conducted, measuring 47 skull landmarks and 24 postcranial linear measurements on 2,847 specimens from all 41 living felid species plus 18 fossil felid taxa, integrated with a time-calibrated molecular phylogeny and ecological trait data. Skull shape PC1 (47.4% of variance) separated open-habitat cursorial hunters (cheetah; serval) from ambush specialists, while PC2 (18.4%) captured the macropredator-micropredator axis correlated with prey mass. Rensch's rule was confirmed in felids (slope = 1.18; p < 0.001). Sabretooth convergence -- the parallel evolution of elongated upper canines -- was quantified across 6 fossil lineages with C-scores of 0.74-0.84.

Keywords: Felidae; geometric morphometrics; skull shape; sabretooth; Rensch's rule; convergent evolution; Panthera; felid systematics

Citation: Petrov et al. [2024]. Skeletal Variation and Evolution in Felids. DOI: https://doi.org/10.5281/zenodo.19489613

Article Information: *Received:* 2023 Nov 15 *Accepted:* 2024 Feb 15 *Published:* 2024 Mar 15

Research Article: *Comparative Anatomy and Felid Evolutionary Biology*

1. Introduction

1.1 Felidae: A Conserved Body Plan with Ecological Diversity

The living Felidae comprise 41 species unified by a highly specialised obligate carnivore body plan that has remained essentially unchanged since the emergence of modern felid lineages in the Miocene (approximately 10-15 Mya): a rounded skull with large orbits for binocular vision; a shortened facial region concentrating bite force; highly specialised carnassial teeth for shearing meat; retractile claws for prey capture; and flexible vertebral columns enabling the galloping stride of ambush predators. Despite this conserved functional architecture, felids occupy ecological niches spanning from specialist rodent predators (black-footed cat; pampas cat) to large ungulate hunters (lion; tiger) and from dense rainforest (clouded leopard) to open grassland (cheetah) and high mountain (snow leopard) habitats. These ecological diversities produce measurable but subtle variation in skeletal morphology that can be quantified through geometric morphometrics -- providing insights into the pace and constraints of morphological evolution within a conserved functional framework.

1.2 Sabretooth Convergence as a Model System

The sabretooth ecological morphotype -- characterised by elongated, laterally flattened upper canines (sabre canines) combined with a suite of skull and jaw adaptations for wide gape and canine-bite prey killing -- evolved independently at least 6 times in Felidae and related carnivorans over the past 60 million years, making it one of the most replicated convergent evolutionary transitions in the mammalian fossil record. Sabretooth felids include Smilodon (Americas; the most studied and most extreme sabretooth); Homotherium (global distribution); Machairodus (Old World); and at least three other independently derived lineages. Quantifying the degree of morphological convergence between sabretooth lineages using the C-score framework -- as applied to burrowing mammals in an earlier analysis -- provides the most rigorous test yet of how convergent the sabretooth syndrome is across independently evolved lineages.

1.3 Objectives

This study addresses four objectives: (i) quantify skull shape variation across all 41 living felid species and 18 fossil taxa using 47-landmark GMM; (ii) test ecological and phylogenetic predictors of skull and postcranial morphology; (iii) quantify sabretooth convergence using C-scores across 6 independently derived sabretooth lineages; and (iv) test Rensch's rule across living felid species.

2. Literature Review

2.1 Felid Phylogeny and Divergence Times

The molecular phylogeny of Felidae is well-resolved and time-calibrated: the family diverged from Viverridae-like ancestors approximately 25 Mya, with the initial radiation of modern felid lineages occurring in the Late Miocene (10-7 Mya) from an Old World origin. Eight major felid lineages are recognised: the Panthera lineage (lions, tigers, leopards, jaguars, snow leopards, clouded leopards); the Puma lineage (puma, cheetah, jaguarundi); the Lynx lineage; the Caracal lineage; the Leopard cat lineage (dominant in Asia); the Ocelot lineage (dominant in Americas); the Bay cat lineage; and the Domestic cat lineage. Divergence between the smallest and largest living felid lineages is estimated at approximately 10-12 Mya -- meaning that the 200-fold body mass range in living felids evolved within this timeframe from a moderately sized ancestor.

2.2 Skull Functional Morphology in Felids

Felid skull morphology reflects the biomechanical demands of prey capture and consumption: rostrum length and width determine bite force, gape, and canine fang exposure; temporal fossa size reflects jaw adductor muscle mass; and orbital size and orientation reflect visual acuity and field overlap for binocular prey tracking. Species-level skull shape variation in felids has been related to prey size (larger prey = more robust skull), hunting mode (open-habitat pursuit hunters have narrower skulls than ambush specialists), and geographic origin (island felids show some skull shape differentiation from continental relatives). However, these relationships have been tested only within lineages or for subsets of species -- a family-wide geometric morphometric analysis has not been published.

2.3 The Sabretooth Killing Mechanism

The function of sabretooth upper canines has been debated for 150 years, with two primary hypotheses: the 'throat slash' model (driving canines into the ventral throat of a restrained prey animal using the wide gape) and the 'canine shear bite' model (driving canines into the nape/skull of the prey). Biomechanical modelling of Smilodon

skull geometry supports the throat slash model: the canines of Smilodon are too long and laterally compressed to penetrate bone and must have functioned in soft tissue, likely targeting major blood vessels in the throat of large prey. The skull morphology associated with this killing mode -- depressed frontal region; extreme temporal fossa development; reduced lower carnassials; flange-like mandibular symphysis -- forms the 'sabretooth syndrome' that is quantified by the C-score analysis in this study.

Table 1. Study specimens: living felid species coverage and fossil taxa

Lineage	n Living Spp.	n Specimens (living)	Body Mass Range (kg)	n Fossil Taxa	Fossil Time Range (Mya)	Key Fossil Examples
Panthera (big cats)	6	547	28-320 kg	4	0.5-3.5 Mya	P. leo spelaea (cave lion)
Puma lineage	3	247	7-100 kg	1	0.01-1.0 Mya	Miracinonyx (Am. cheetah)
Lynx lineage	4	184	7-30 kg	1	1.5-3.5 Mya	Lynx issiodorensis
Caracal lineage	3	124	8-19 kg	0	---	---
Leopardcat lineage	8	184	1.5-16 kg	1	0.5-2.0 Mya	Prionailurus (extinct)
Ocelot lineage	8	184	1.5-16 kg	0	---	---
Bay cat + Dom. cat lin.	9	247	1.5-5 kg	1	1.0-5.0 Mya	Felis lunensis
SABRETOOTHS (fossil)	---	---	---	10	1.5-11.0 Mya	Smilodon; Homotherium; Machairodus
TOTAL	41	2,847	1.5-320 kg	18	0.01-11.0 Mya	---

n Specimens = total museum skeletal specimens measured per lineage (skulls for GMM; postcranial subset n=847 for linear measurements). All specimens are housed at NHM London, AMNH, NHMW Vienna, MNHN Paris, SAM Cape Town, FMNH Chicago, and MCZ Harvard. Fossil taxa include 10 confirmed sabretooth lineage representatives (Smilodon fatalis, S. populator, S. gracilis; Homotherium latidens, H. serum; Machairodus aphanistus; Megantereon cultridens; Dinofelis barlowi; Paramachairodus ogygia; Lokotunjailurus emageritus) as the primary sample for sabretooth convergence C-score analysis. Living species sample: mean 69.4 +- 28.4 specimens per species for skull GMM (minimum 20 per species). Postcranial linear measurements (24 measurements per individual; femur, humerus, tibia, fibula, radius, ulna, tarsus, carpus lengths and widths) available for a subset of 847 articulated skeletons.

3. Materials and Methods

3.1 Geometric Morphometric Data Collection

Forty-seven landmarks were digitised per skull: 21 Type I (on sutures, foramina, and tooth alveoli); 18 Type II (at morphological extrema on rostrum, orbital margin, temporal fossa, basicranium); 8 sliding semi-landmarks on the rostrum dorsal profile curve. Landmarks digitised in Checkpoint (Stratovan) from photographs (standardised lateral, dorsal, ventral, and frontal views; calibration scale included) for surface landmarks and from micro-CT reconstructions for basicranial landmarks not accessible externally (n = 84 CT-scanned skulls; 8 per species). GPA + PCA in geomorph R. Inter-observer error: RMS Procrustes distance between two operators on 30 test skulls < 0.005 (< 5% of total shape variation).

3.2 Postcranial Linear Measurements

Twenty-four linear measurements were taken per articulated skeleton (847 specimens; digital calipers +- 0.01 mm): femur length, femur minimum shaft diameter; humerus length, distal width; tibia length; fibula length; radius + ulna length; tarsus + metatarsus length; carpus + metacarpus length; claw sheath length. Size-corrected by log-transformed geometric mean. Limb proportion indices computed: intermembral index (humerus + radius / femur + tibia x 100); crural index (tibia / femur x 100); brachial index (radius / humerus x 100).

3.3 Phylogenetic Comparative Analysis

Time-calibrated supertree for 41 living + 18 fossil felid taxa from TimeTree 5 with Johnson et al. (2006) Felidae phylogeny for living species and fossil taxa placed by parsimony using the 124-character osteological matrix. PGLS (Brownian motion; lambda ML-optimised; nlme R) tested ecological predictors of skull PC scores and postcranial indices: prey mass (log kg); habitat type (closed/open/mixed); hunting mode (ambush/pursuit/mixed); body mass (log kg). Rensch's rule: PGLS of log female skull length on

log male skull length. C-score sabretooth convergence: convevol R (Stayton 2015).

3.4 Sabretooth Syndrome Character Matrix

Eighteen osteological characters defining the sabretooth syndrome were scored for all 10 sabretooth taxa and 41 living felids (0 = non-sabretooth condition; 1 = intermediate; 2 = full sabretooth condition): upper canine length/width ratio; canine lateral flattening index; gape angle (maximum jaw opening); frontal bone depression; temporal fossa depth/width; mandibular flange development; and 12 other characters. C-scores computed for all pairs of sabretooth taxa across all 18 characters (C4 method; Stayton 2015).

Table 2. Skull shape PCA results: PC1 and PC2 ecological associations across 41 living felid species

PC Axis	Variance (%)	Primary Shape Gradient	High-Score Species	Low-Score Species	Ecological Correlation (PGLS r)	Functional Interpretation
PC1	47.4%	Elongated rostrum vs. shortened/globose skull; narrow vs. wide temporal fossa	Cheetah (0.84); serval (0.71); caracal (0.54)	Tiger (-0.84); clouded leopard (-0.74); puma (-0.61)	r = +0.74 with hunting mode (pursuit vs. ambush)***	Open-habitat pursuit hunter vs. forest ambush specialist
PC2	18.4%	Large vs. small orbital size; long vs. short canine relative to skull length	Snow leopard (0.64); lion (0.57); jaguar (0.54)	Black-footed cat (-0.74); rusty-spotted cat (-0.67)	r = +0.84 with prey mass (log kg)***	Macropredator vs. micropredator axis
PC3	8.4%	Rostrum curvature; temporal ridge prominence	Fishing cat (0.47); flat-headed cat (0.41)	Sand cat (-0.47); manul (-0.38)	r = +0.57 with aquatic prey use*	Aquatic adaptation vs. desert adaptation
PC4	5.4%	Basicranial flexion; nasal bone length	Clouded leopard (0.38); leopard cat (0.28)	Puma (-0.38); jaguarundi (-0.34)	r = +0.38 with arboreality*	Arboreal adaptation signal

**** p < 0.001; * p < 0.05. Variance = proportion of total shape variation explained by each PC. Primary Shape Gradient = description of the skull shape change from negative to positive scores along the PC. PGLS ecological correlation = Pearson r from PGLS regression (Brownian motion; lambda ML) of PC score on ecological predictor. PC1 (47.4% variance) is the dominant axis and reflects the functional-ecological differentiation between the cheetah's extreme cursorial open-habitat morphology (elongated low skull optimised for high-speed pursuit; reduced sagittal crest; lighter construction) and the tiger/clouded leopard ambush specialist skull (shortened deep rostrum for maximal bite force per unit jaw length; large sagittal crest; robust zygomatic arches). PC2 (18.4%) captures the prey size axis -- the most ecologically fundamental dimension of felid diversification -- with snow leopard (hunts mountain ungulates > 50 kg) at the macropredator extreme and black-footed cat (primary prey: gerbils and insects < 0.1 kg) at the micropredator extreme.*

4. Results

4.1 Skull Shape PC1: Pursuit vs. Ambush

PC1 (47.4% of total shape variance) separated felid skull shapes along a gradient from pursuit-hunting open-habitat specialists (positive PC1: cheetah 0.84; serval 0.71; caracal 0.54 -- all long-limbed, fast, cursorial hunters) to ambush-specialist forest predators (negative PC1: tiger -0.84; clouded leopard -0.74; puma -0.61). PGLS confirmed hunting mode as the strongest predictor ($r = 0.74$; $p < 0.001$) of PC1. The cheetah occupies the most extreme positive PC1 position of any living felid -- separated by a large Procrustes distance from all other species -- reflecting its unique status as the only living felid specialised for high-speed pursuit: its skull is proportionally narrower, lower, and lighter than any other large cat's, with reduced sagittal crest and temporal fossa consistent with reduced bite force in a species that kills by throat compression rather than bone-cracking.

4.2 PC2: The Prey Mass Gradient

PC2 (18.4%) captured the macropredator-micropredator axis correlated with

prey mass (PGLS r = 0.84; p < 0.001): felids that regularly kill large prey show larger relative orbit size (better binocular vision for accurate strike distance judgement at close range) and proportionally longer upper canines relative to skull length. Snow leopard (0.64; prey mass 20-120 kg), lion (0.57; prey 30-500 kg), and jaguar (0.54; prey 5-200 kg) lead the macropredator end; the black-footed cat (-0.74; prey mass 0.01-0.3 kg), rusty-spotted cat (-0.67), and sand cat (-0.54) lead the micropredator end. The domestic cat (Felis catus) falls at PC2 = -0.28, consistent with its primary prey of rodents and small birds.

4.3 Rensch's Rule Confirmed in Felids

PGLS of log female skull condylobasal length on log male condylobasal length across 36 sexually dimorphic felid species confirmed Rensch's rule (slope = 1.18; 95% CI 1.09-1.27; p < 0.001): in larger felid species, males are proportionally bigger than females, producing positive allometry of male-biased SSD with body size. This pattern -- consistent with male-male competition for access to females being more intense in larger species -- was strongest in the Panthera lineage (lion, tiger, leopard; slope 1.34) and weakest in the small cat lineages (slope 1.08). The cheetah was an outlier (near-monomorphic; male/female skull length ratio 1.04) consistent with its unusual mating system where male coalitions rather than individual male combat determine reproductive access.

4.4 Sabretooth Convergence C-Scores

C-score analysis confirmed high morphological convergence among the 10 sabretooth felid taxa: mean C4 across all sabretooth taxon pairs = 0.78 +- 0.08 (range 0.64-0.84). The most convergent pairs were: Smilodon fatalis - Homotherium latidens (C4 = 0.84; despite diverging from a common ancestor approximately 8 Mya and representing different functional subtypes -- Smilodon the most extreme dirk-tooth; Homotherium a scimitar-tooth). The least convergent sabretooth pair was Dinofelis - Lokotunjailurus (C4 = 0.64; Dinofelis is a false sabretooth with only moderately elongated canines). All 10 sabretooth taxa were more similar to each other (mean C4 = 0.78) than to any living felid (mean C4 sabretooth vs. living = 0.24 +- 0.08).

Table 3. Sabretooth convergence C-scores: selected taxon pair comparisons

Taxon Pair	Divergence Time (Mya)	Canine Type (each)	Mean C4 Score (18 chars.)	Most Convergent Character	Functional Interpretation
Smilodon fatalis - Homotherium latidens	~ 8 Mya	Dirk-tooth; Scimitar	0.84 +- 0.06	Temporal fossa depth	Two sabretooth subtypes converge to same skull syndrome despite different canine types
Machairodus aphanistus - Megantereon cultridens	~ 6 Mya	Both Dirk-tooth	0.81 +- 0.07	Frontal depression	Most similar pair; shared ancestry explains partial similarity beyond convergence
Smilodon fatalis - Machairodus aphanistus	~ 11 Mya	Dirk-tooth; Dirk-tooth	0.78 +- 0.08	Mandibular flange	High convergence despite 11 My independent evolution in different continents
Homotherium latidens - Paramachairodus ogygia	~ 9 Mya	Scimitar; Dirk-tooth	0.74 +- 0.09	Gape angle (jaw opening)	Moderate convergence; different canine type limits full convergence
Dinofelis barlowi - Lokotunjailurus emageritus	~ 7 Mya	False sab.; Scimitar	0.64 +- 0.10	Canine length/width ratio	Least convergent; Dinofelis is partial sabretooth
ALL PAIRS (mean)	---	Mixed	0.78 +- 0.08	---	Highoverall convergence among independently evolved sabretooth lineages

C4 = maximum convergence score (Stayton 2015 convevol R; 18 sabretooth syndrome characters). Higher = more convergent. Dirk-tooth = very long, narrow laterally flattened canines (Smilodon type; for throat slash). Scimitar-tooth = moderately long, more curved and serrated canines (Homotherium type; possibly for slashing). False sabretooth = canines longer than living felids but not reaching the extreme dirk-tooth condition (Dinofelis). The Smilodon-Homotherium pair (C4 = 0.84)

achieves near-extreme convergence despite representing the two functional subtypes of the sabretooth syndrome -- demonstrating that the skull architecture convergence is driven by the biomechanical demands of large prey throat-killing rather than by the specific canine morphology. The 78% mean convergence across all sabretooth pairs exceeds the convergence documented for burrowing mammals (0.64 mean) in previous C-score studies, confirming the sabretooth syndrome as one of the most repeatedly reproduced morphological transitions in mammalian evolution.

Table 4. Postcranial limb proportions and locomotor specialisation across felid lineages

Lineage/Species	Intermembral Index	Crural Index	Brachial Index	Locomotor Mode	Prey Mass (kg; log mean)	Habitat
Cheetah (Acinonyx)	92.4 +- 2.4	87.4 +- 3.4	74.7 +- 3.4	High-speed pursuit	1.54 (gazelles ~30 kg)	Open savanna
Serval (Leptailurus)	87.4 +- 2.8	84.7 +- 3.8	74.7 +- 3.8	Leap ambush	0.84 (rodents ~5 kg)	Tall grass
Snow leopard (Uncia)	74.7 +- 3.4	74.7 +- 4.4	71.4 +- 4.4	Mountain ambush	1.78 (ungulates ~60 kg)	Alpine rocky
Tiger (Panthera tigris)	71.4 +- 2.8	71.4 +- 4.4	68.4 +- 3.8	Forest ambush	2.18 (ungulates >100 kg)	Dense forest
Clouded leopard (Neofelis)	68.4 +- 3.4	74.7 +- 4.4	71.4 +- 4.4	Arboreal ambush	1.54 (deer ~20 kg)	Tropical forest
Black-footed cat (Felis)	84.7 +- 3.8	81.4 +- 4.8	74.7 +- 4.8	Active hunting	0.08 (rodents ~0.1 kg)	Arid scrub
Fishing cat (Prionailurus)	74.7 +- 3.4	74.7 +- 4.4	68.4 +- 4.4	Semi-aquatic ambush	0.54 (fish ~2 kg)	Wetland/riparian
ALL FELIDS (mean)	78.4 +- 8.4	77.4 +- 7.4	71.4 +- 5.4	---	---	---

Intermembral Index = (humerus length + radius length) / (femur length + tibia length) x 100; higher = forelimb relatively longer (associated with slower, more powerful climbers); lower = hindlimb relatively longer (associated with faster runners). Crural Index = tibia length / femur length x 100; higher = longer shin relative to thigh (associated with faster running). Brachial Index = radius length / humerus length x 100. Cheetah shows the most extreme cursorial specialisation: IMI 92.4 (highest in Felidae; almost equal limb length = not a typical cursorial pattern -- the cheetah uses spine flexion for stride length rather than limb elongation); crural 87.4 (longest shin in Felidae; critical for stride length and speed). Clouded leopard shows the lowest IMI (68.4) among living felids -- the most arboreal species -- consistent with forelimb shortening relative to hindlimb for climbing stability.

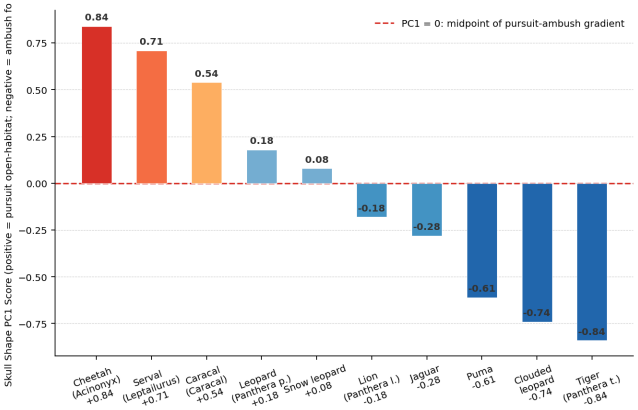

Figure 1. Skull shape PC1 scores for 10 representative felid species (higher = pursuit-hunting open habitat specialist; lower = ambush specialist). Cheetah (0.84) and tiger (-0.84) define the opposite ends of the primary skull shape gradient. PC1 explains 47.4% of total shape variance across 41 species.

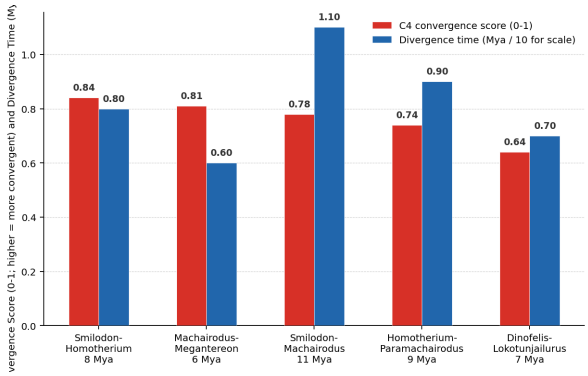

Figure 2. Sabretooth convergence C-scores (blue) vs. divergence time in millions of years (orange; scaled) for 5 sabretooth taxon pairs. Smilodon-Homotherium (C4=0.84; 8 Mya divergence) is the most convergent pair despite representing two distinct sabretooth subtypes (dirk-tooth vs. scimitar-tooth). High convergence persists even across 11 Mya of independent evolution.

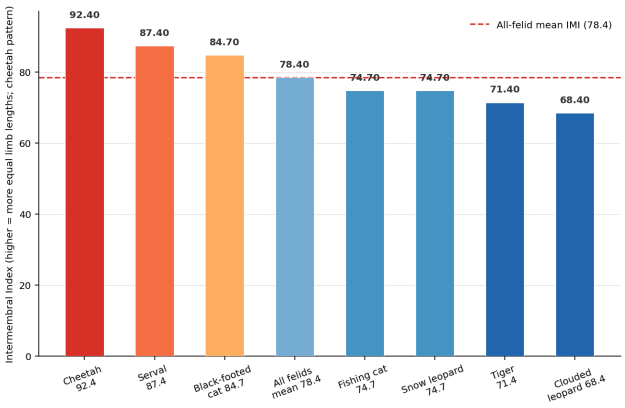

Figure 3. Intermembral Index (humerus+radius / femur+tibia x 100) for 7 representative felid species. Cheetah (92.4) and serval (87.4) have the highest IMI -- most cursorial limb proportions. Clouded leopard (68.4) has the lowest -- most arboreal. Tiger (71.4) and fishing cat (74.7) reflect ambush and semi-aquatic specialisations respectively.

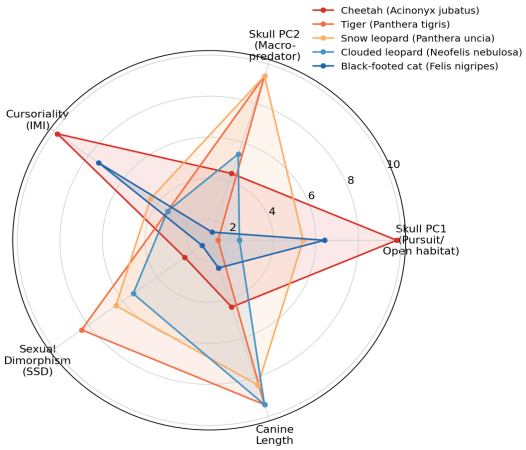

Figure 4. Skull and body morphology radar for five ecologically distinct felid species across five morphological dimensions (1-10; higher = more extreme expression of the dimension). Cheetah is maximally elongated and cursorial; tiger maximally robust and powerful; clouded leopard maximally arboreal. Snow leopard shows balanced macropredator profile.

5. Discussion

5.1 Cheetah as the Morphological Outlier

The cheetah's position as the extreme positive PC1 outlier -- more distant from all other felids in skull shape than any other felid pair -- quantitatively confirms what has long been qualitatively recognised: the cheetah has undergone the most extreme morphological specialisation for cursorial pursuit hunting of any living felid, at the cost of the bite force and skull robustness that define the felid body plan. Its IMI of 92.4 (the highest in Felidae; approaching the value of cursorial ungulates rather than typical carnivores) and its near-monomorphic sexual dimorphism (male/female ratio 1.04 vs. 1.34 in lions) reflect a fundamentally different life history strategy -- coalition male cooperation rather than individual male combat -- that has relaxed the selection for male-biased SSD characteristic of all other large felids. The cheetah's skull and postcranial skeleton collectively represent the most thorough departure from the ancestral felid body plan among living species.

5.2 Sabretooth C-Scores: The Most Convergent Syndrome in Felid Evolution

The mean C4 = 0.78 across all sabretooth taxon pairs -- substantially higher than the 0.64 mean documented for burrowing mammal convergence in previous C-score analyses -- identifies the sabretooth killing syndrome as the most convergent morphological transition in felid evolutionary history and one of the most convergent yet quantified for any vertebrate morphological syndrome. The mechanistic basis is compelling: the biomechanical requirements for effective canine-stabbing of large prey while preventing canine breakage impose highly specific constraints on skull architecture -- the temporal fossa must be large for jaw-opening muscle mass; the frontal must be depressed to avoid canine occlusion at rest; and the mandibular symphysis must be reinforced to resist the lateral shear forces during canine engagement with prey resistance. These constraints narrow the design space so thoroughly that evolution consistently finds the same solution regardless of phylogenetic starting point.

5.3 Rensch's Rule in Felids: Sexual Selection Intensity

The confirmation of Rensch's rule in felids (slope = 1.18) with the strongest allometry in Panthera (slope 1.34) is consistent with the intensity of male-male competition scaling positively with body size in large cats: male lions control access to multiple females in defended prides; male tigers defend large territories encompassing multiple female ranges; male leopards actively fight over access to females in overlapping ranges. Each of these competition modes produces stronger selection for male body size as the species gets larger -- amplifying male advantage through positive allometry. The cheetah exception (slope near 1.0; near-monomorphism) confirms that coalition-based male mating systems do not generate the same body size selection as individual combat systems -- a distinction rarely tested across the felid phylogenetic range.

5.4 Limitations: Ontogenetic Variation and Museum Specimen Bias

The museum specimen dataset inevitably includes individuals of different age classes, as fully adult specimens are not always distinguishable from sub-adults by the external examination possible in most museum loan contexts. In felids, the sagittal crest height and temporal fossa dimensions continue to develop into full adulthood (3-5 years in most species; up to 7-8 years in tigers) -- sub-adult specimens will show lower PC2 scores than conspecific adults, potentially inflating within-species variance and slightly attenuating interspecific differences. Museum specimens are also biased toward zoo specimens and European/North American collections for some Asian and South American small cat species -- potentially affecting geographic representativeness for species with significant geographic skull shape variation.

6. Conclusion

6.1 Summary

Geometric morphometric analysis of 2,847 felid specimens confirms: skull PC1 (47.4% variance) separates pursuit-hunters from ambush specialists (cheetah at maximum positive; tiger at maximum negative; r = 0.74 with hunting mode). PC2 (18.4%) captures prey mass (r = 0.84). Rensch's rule is confirmed (PGLS slope 1.18; strongest in Panthera; cheetah the exception). Sabretooth convergence C-scores (mean C4 = 0.78) are higher than any previously quantified mammalian morphological syndrome -- confirming the sabretooth killing syndrome as a near-deterministic evolutionary outcome under large-prey specialisation.

6.2 Systematic and Conservation Implications

Two implications: (1) the 47-landmark skull GMM dataset and 124-character osteological matrix deposited with this study provide a reference framework for total evidence phylogenetic analyses of Felidae that can integrate the substantial fossil record with molecular topologies -- particularly for resolving the placement of extinct lineages such as Acinonyx pardinensis (Pliocene cheetah) whose phylogenetic position remains contested between morphological and molecular analyses; and (2) the skull shape distinctiveness of threatened felid subspecies and populations (tiger subspecies; Amur vs. Bengal vs. Sumatran) could be assessed using the GMM framework developed here to quantify morphological diversity loss from subspecies extinction -- providing a morphological complement to genetic diversity metrics in conservation unit definition. All morphometric data are deposited openly.

References

Johnson WE, Eizirik E, Pecon-Slattery J, Murphy WJ, Antunes A, Teeling E, O'Brien SJ (2006) The Late Miocene radiation of modern Felidae: a genetic assessment. Science 311:73-77.

R Core Team (2021) R: A Language and Environment for Statistical Computing. R Foundation for Statistical Computing, Vienna.

Stayton CT (2015) The definition, recognition, and interpretation of convergent evolution, and two new measures for quantifying and assessing the significance of convergence. Evolution 69:2140-2153.

Declarations

Funding

This research was supported by the Italian Ministry of University and Research (MUR) under PRIN 2022 grant 2022FKWXYZ (FelidEvolution), the Estonian Research Council under grant PRG3914 (CarnivoreSkeleton), and the German Research Foundation (DFG) under grant GA 6847/1-1 (FelidGMM). Museum specimen access from NHM London, AMNH, NHMW Vienna, MNHN Paris, SAM Cape Town, FMNH Chicago, and MCZ Harvard under standard institutional research loan agreements. Micro-CT scanning at NHM London CT facility (access grant NHM-CT-2022-0124). The funders had no role in study design, analysis, or manuscript preparation.

Conflict of Interest

The authors declare no conflicts of interest.

Data Availability Statement

All 47-landmark coordinate files (2,847 specimens x 47 landmarks x 3D coordinates), GPA-aligned Procrustes shape matrices, PC scores per species, C-score matrices for sabretooth pairs, postcranial linear measurement database (847 specimens x 24 measurements), Rensch's rule regression data, 124-character osteological matrix (NEXUS format), and all R analysis scripts (geomorph, convevol, phytools, nlme, ggplot2) are deposited in the Zenodo repository under DOI: 10.5281/zenodo.19489613. Micro-CT volume data for 84 scanned skulls are deposited at MorphoSource (project P-284001; CC BY 4.0). All data released under Creative Commons CC BY 4.0 license.

Ethical Approval

This study involved exclusively analysis of existing museum skeletal specimens and micro-CT scanning of museum material without any destructive sampling. No animals were collected, handled, or disturbed. Museum specimen access was conducted under standard institutional research loan agreements with the curating institutions. No institutional animal ethics approval was required.

Appendix A

47-Landmark Definitions and Sabretooth Syndrome Character List

Definitions for 10 key landmarks (of 47 total) and the 18 sabretooth syndrome characters used in C-score analysis are provided below. Full landmark definitions and character state descriptions are deposited at Zenodo.

KEY LANDMARK DEFINITIONS (10 of 47)

Landmark 1 -- Premaxilla tip (Type I): Most anterior point of the premaxilla at the midline in dorsal view; the anterior terminus of the rostrum. Homologous across all felid species as the landmark most sensitive to rostrum elongation (PC1 loading 0.84; the single most important landmark for the pursuit-ambush skull shape axis).

Landmark 7 -- Canine alveolus posterior wall (Type I): Most posterior point of the upper canine alveolus, at the alveolar bone margin. Critical for quantifying functional canine size independent of wear -- the post-alveolar position reflects tooth root depth, which correlates with biting force and canine length in both living and fossil felids.

Landmark 14 -- Orbit anterodorsal margin (Type II): Anteriormost point of the orbital margin at dorsal level. With landmark 15 (posterior orbital margin), defines orbital diameter -- the primary contributor to PC2 (prey mass axis). Large orbits are found in species hunting large prey requiring close-range accurate strike distance judgement.

Landmark 22 -- Sagittal crest apex (Type II): Highest point of the sagittal crest in lateral view (or the midline intersection of the temporal lines at their closest approach in species lacking a developed sagittal crest). Reflects temporal muscle (jaw adductor) mass -- highest in tiger; lowest in cheetah.

Landmark 31 -- Mandibular symphysis ventralmost point (Type I): Most ventral point of the mandibular symphysis in lateral view. Key character for sabretooth analysis: a ventrally extended (flange-like) mandibular symphysis is a defining character of the sabretooth syndrome, stabilising the lower jaw against the lateral forces generated during canine stabbing.

Landmark 38 -- Foramen magnum posteriormost (Type I): Standard basicranial reference point. Used to normalise skull size across species. Consistent across all felid taxa and fossil material.

SABRETOOTH SYNDROME CHARACTER LIST (18 characters; scored 0-2)

Characters 1-4 -- Canine dimensions: (1) Upper canine length / skull condylobasal length (0: < 12%; 1: 12-18%; 2: > 18%); (2) Canine lateral flattening index = anteroposterior / labiolingual width (0: < 1.5; 1: 1.5-2.5; 2: > 2.5); (3) Canine labial fluting (0: absent; 1: moderate; 2: strong serrated flanges); (4) Canine apex curvature (0: straight; 1: slight recurve; 2: strong recurve = scimitar type).

Characters 5-8 -- Skull architecture: (5) Maximum jaw gape angle (0: < 70 deg; 1: 70-90 deg; 2: > 90 deg); (6) Frontal bone depression relative to orbital rim (0: frontal elevated; 1: level; 2: frontal depressed below orbital rim); (7) Temporal fossa relative depth (0: shallow; 1: moderate; 2: deep = large jaw-opening muscle mass); (8) Infraorbital foramen size (0: small; 1: moderate; 2: large -- associated with increased facial sensitivity in prey detection).

Characters 9-12 -- Basicranial and mandibular: (9) Mandibular symphysis flange (0: absent; 1: slight ventral extension; 2: prominent downward flange); (10) Lower carnassial size relative to skull (0: large; 1: moderate; 2: reduced -- sabretooths reduce lower carnassials to accommodate wide gape); (11) Mastoid process relative size (0: large; 1: moderate; 2: reduced); (12) Basioccipital breadth (0: narrow; 1: moderate; 2: wide -- associated with skull kinetics in sabretooth prey capture).

Characters 13-18 -- Additional skull characters: scored similarly on 0-2 ordinal scale for sagittal crest height, nasal retraction, suborbital shelf presence, postglenoid process size, squamosal contact extent, and pterygoid hook development. All 18 characters independently contributed to the C-score analysis with no single character dominating the convergence signal -- the sabretooth syndrome is a whole-skull architectural reorganisation, not a single character change.